UNIVERSITY
OF TRENTO

DIPARTIMENTO DI INGEGNERIA E SCIENZA DELL'INFORMAZIONE

38123 Povo – Trento (Italy), Via Sommarive 14
http://www.disi.unitn.it

MULTI-FREQUENCY/MULTI-SCALING TECHNIQUES FOR THE ELECTROMAGNETIC INVERSION OF LOSSLESS PROFILES – A NUMERICAL COMPARISON

D. Franceschini, M. Donelli, G. Franceschini, A. Massa

January 2011

Technical Report # DISI-11-233

Multi-Frequency/Multi-Scaling Techniques for the Electromagnetic Inversion of Lossless Profiles - A Numerical Comparison

D. Franceschini, M. Donelli, G. Franceschini, and A. Massa

Department of Information and Communication Technology
University of Trento, Via Sommarive 14, 38050 Trento, Italy
{davide.franceschini, massimo.donelli, gabriele.franceschini}@dit.unitn.it, andrea.massa@ing.unitn.it

Abstract: Starting from the iterative multi-scaling approach developed for monochromatic illuminations, two multi-resolution strategies have been studied for dealing with multi-frequency inverse scattering experiments. The first approach is based on a multi-scaling frequency-hopping reconstruction scheme, while the second one is concerned with a simultaneous multi-resolution processing of multi-frequency data. In this contribution, a comparative assessment is performed by means of a set of representative experiments in order to evaluate the reconstruction accuracies of the proposed implementations also in comparison with the monochromatic multi-step process.

Keywords: Electromagnetic Inverse Scattering, Multi-Frequency Data, Iterative Multi-Scaling Approach, Multi-Resolution Techniques.

1. Introduction

The electromagnetic properties of an inaccessible area of investigation can be obtained in a non-invasive fashion by means of microwave imaging techniques [1]-[4].

One of the main problems in processing scattered electromagnetic radiations is related to the intrinsic limitations of the collectable information on the scenario under test. As a matter of fact, it has been shown [5] that an oversampling of the scattered field does not arbitrarily increase the information content of the measures and thus, since single-illumination measurement setups do not usually allow an accurate reconstruction of the scatterers, multi-view and multi-illumination acquisition setups have been proposed [6]. Moreover, an enhanced reconstruction accuracy can be obtained by using frequency-hopping strategies (e.g., [7]) or simultaneously processing multi-frequency data [8]-[10]. Unfortunately, when dealing with multi-frequency data, one has to consider the growing necessity (with respect to the monochromatic case) of computational and storage resources.

As far as the problem unknowns are concerned, the object function that models the electromagnetic behavior of the unknown object depends on the working frequency, but suitable countermeasures can be adopted to limit the increase of the unknown space. As an example, the Maxwellian model defines a relationship between the contrast at a reference frequency and those at different frequencies (e.g., [8] and [9]).

In the framework of multi-frequency inversion algorithms, few works has investigated the exploitation of multi-frequency data through multi-resolution strategies [11]. This contribution is aimed at preliminary analyzing two multi-frequency approaches integrated into a multi-step inversion algorithm (IMSA) [12][13] previously applied to monochromatic data. As a matter of fact, non-negligible advantages are expected

exploiting the benefits of a multi-resolution expansion of the unknowns in the presence of an enlarged set of information coming from the multi-frequency experiments.
An outline of the paper is as follows. Sections 2 briefly summarizes the key-features of the proposed multi-frequency/multi-resolution approaches. A numerical validation will follow together with a comparative analysis (Sect. 3). Finally, some comments and conclusions will be reported (Sect. 4).

2. Mathematical Formulation

Let us refer to a two-dimensional geometry (Fig. 1) characterized by an inhomogeneous cross section D lying in a homogeneous host medium, which is assumed to be the vacuum. Such a scenario is illuminated by a set of *P* monochromatic (f_p being the working frequency of the p-th illumination, $p = 1,...,P$) incident electric fields *TM*-polarized impinging from *V* different directions ($E_{v,p}^{inc}(x,y)\hat{\mathbf{z}}$, $v = 1,...,V$, $p = 1,...,P$).

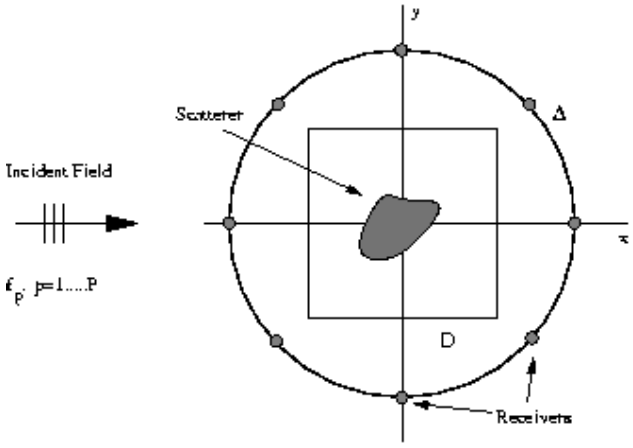

Figure 1. Geometry of the problem.

The reconstruction of the frequency-dependent contrast function

$$\tau_p(x,y) = \varepsilon_r(x,y) - 1 - j\frac{\sigma(x,y)}{2\pi f_p \varepsilon_0} \quad p = 1,...,P \tag{1}$$

expressed in terms of the relative permittivity, $\varepsilon_r(x,y)$, and the conductivity, $\sigma(x,y)$, of the medium, is carried out exploiting the multi-frequency information available from the scattered field $E_{v,p}^{scatt}(x_{m_{v,p}}, y_{m_{v,p}})\hat{\mathbf{z}}$, collected at $m_{v,p} = 1,...,M_{v,p}$ measurement points belonging to an observation domain Δ.
The physical relation between the contrast function $\tau_p(x,y)$ and the scattering data (namely, the scattered field in the observation domain, $E_{v,p}^{scatt}(x_{m_{v,p}}, y_{m_{v,p}})$, $(x_{m_{v,p}}, y_{m_{v,p}}) \in \Delta$, and the incident field in the investigation domain, $E_{v,p}^{inc}(x,y)$, $(x,y) \in D$) is provided by a set of integral equations [12]

$$E_{v,p}^{scatt}(x_{m_{v,p}}, y_{m_{v,p}}) = \Theta_{v,p}^{ext}\left\{\tau_p(x,y)E_{v,p}^{tot}(x,y)\right\} \qquad (x,y) \in D \qquad (x_{m_{v,p}}, y_{m_{v,p}}) \in \Delta \tag{2}$$

$$E_{v,p}^{inc}(x,y) = E_{v,p}^{tot}(x,y) - \Theta_{v,p}^{\text{int}}\left\{\tau_p(x,y)E_{v,p}^{tot}(x,y)\right\} \qquad (x,y) \in D \tag{3}$$

where $\Theta_{v,p}^{ext}$ and $\Theta_{v,p}^{\text{int}}$ denote the external and internal scattering operator, respectively.
In order to effectively deal with multi-frequency data by solving (2) and (3), thus determining the unknown contrast function $\tau_p(x,y)$, the *IMSA* [12] has been suitably modified. In the following, two different inversion techniques (Fig. 2) based on the multi-step/multi-resolution approach are described.

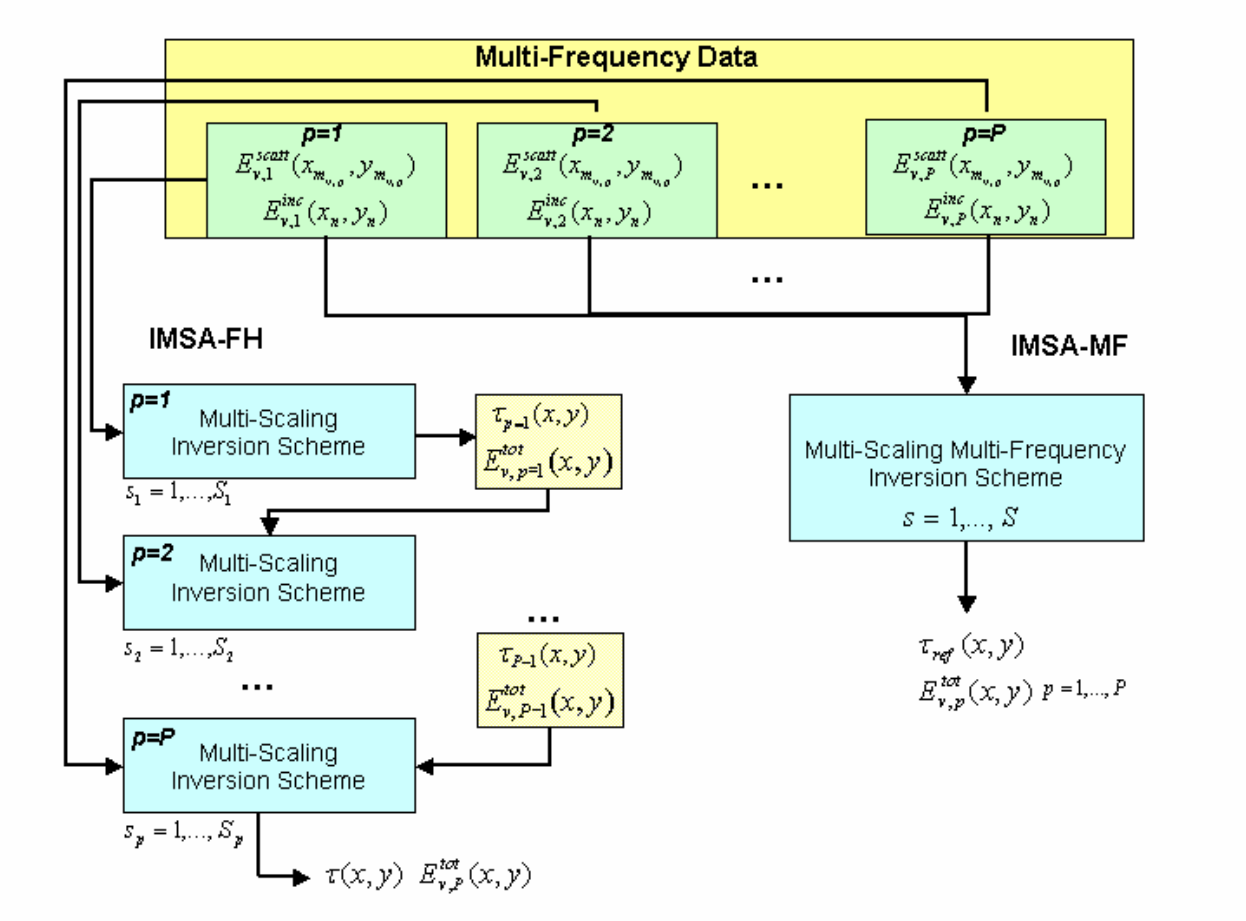

Figure 2. Scheme of the proposed frequency hopping and multi-frequency inversion strategies.

The first inversion procedure is developed integrating a frequency hopping scheme with the *IMSA* in order to process the multi-frequency data one-by-one starting from the lowest available frequency ($f = f_1$). Each stage ($p = 1,\ldots,P$) of the hopping strategy (*IMSA-FH*) consists of a multi-scaling process of S_p optimization steps (Fig. 2).
The key points of the frequency-hopping reconstruction loop ($p = 1,\ldots,P$) can be summarized as follows:

- *Initialization* ($s_p = 0$). The information content of the scattered field [9] at $f = f_p$ is taken into account for partitioning the investigation domain D into N_p sub-domains. Consequently, a suitable set of rectangular basis functions [$\Omega_n(x,y)$, $n = 1,\ldots,N_p$] is defined and the problem unknowns are initialized to the free-space configuration if $p = 1$. In the successive steps, the

profile reconstructed at the convergence step of the $(p-1)$ -th frequency stage is suitably mapped into the investigation domain by setting $E^{tot}_{v,p,s_s=0}(x,y) = E^{tot}_{v,p-1}(x,y)$ and $\tau_{p,s_p=0}(x,y) = \tau_{p-1}(x,y)$;

- *Low-Order Reconstruction* ($s_p = 1$). A homogeneous coarse profile reconstruction is obtained through the minimization of the low-order cost function

$$\Psi_p^{(1)} = \frac{\sum_{v=1}^{V}\sum_{m_{v,p}=1}^{M_{v,p}} \left| E^{scatt}_{v,p}(x_{m_{v,p}}, y_{m_{v,p}}) - \Theta^{ext}_{v,p}\left[\tau_{p,1}(x_n,y_n), E^{tot}_{v,p,1}(x_n,y_n)\right] \right|^2}{\sum_{v=1}^{V}\sum_{m_{v,p}=1}^{M_{v,p}} \left| E^{scatt}_{v,p}(x_{m_{v,p}}, y_{m_{v,p}}) \right|^2} + \frac{\sum_{v=1}^{V}\sum_{n=1}^{N_p} \left| E^{inc}_{v,p}(x_n,y_n) - E^{tot}_{v,p,1}(x_n,y_n) + \Theta^{\mathrm{int}}_{v,p}\left[\tau_{p,1}(x_n,y_n), E^{tot}_{v,p,1}(x_n,y_n)\right] \right|^2}{\sum_{v=1}^{V}\sum_{n=1}^{Np} \left| E^{inc}_{v,p}(x_n,y_n) \right|^2} \tag{4}$$

- *Multi-Scaling Profile Reconstruction* ($s_p = 2,\ldots,S_p$). Starting from the solution estimated at the ($s_p - 1$)-th step, a set of Q^{s_p} regions-of-interest (RoIs), $D^{(q)}_{s_p-1}$, is determined [13] where the resolution level is increased by defining a new set of N_p basis functions whose supports overlap the *RoI*s. Therefore a multi-resolution representation of the unknowns is looked for as the minimum of a multi-resolution cost function detailed in [13];

- *Convergence Assessment*. A set of stability criteria on the reconstruction [13] determines the termination of the multi-scale process and the solution of the P-th frequency stage is assumed as the problem solution.

The second inversion scheme (*IMSA-MF*) is a generalization to multi-frequency data of the *IMSA* strategy proposed in [12], [13] for single-frequency experiments. Firstly, some assumptions on the dispersion relation of the contrast function (1) are done that allow stating the following relationship

$$\tau_p(x,y) = \mathrm{Re}\left\{\tau_{ref}(x,y)\right\} + f\,\frac{f_{ref}}{f_p}\,\mathrm{Im}\left\{\tau_{ref}(x,y)\right\} \tag{5}$$

that relates the value of the contrast at the *p*-th frequency to that at the reference frequency f_{ref}, thus limiting the increasing of the number of unknowns. Therefore, τ_{ref} is the only contrast unknown to be determined as well as the internal fields, $E^{tot}_{v,p}(x,y)$, $p = 1,\ldots,P$, to be estimated for each working frequency of the illumination setup.

As far as the multi-frequency reconstruction loop is concerned, the procedure is similar to that of the standard monochromatic *IMSA* where a multi-scaling procedure of *S* ($s = 1,\ldots,S$) steps is performed for defining the multi-resolution expansion of the unknown parameters

$$\tau_{ref}(x,y) = \sum_{r_s=1}^{R_s}\sum_{n(r_s)=1}^{N(r_s)} \tau_{ref}(x_{n(r_s)}, y_{n(r_s)})\,\Omega_{n(r_s)}(x,y), \qquad R_s = s$$

(6)

$$E_{v,p}^{tot}(x,y)=\sum_{r_s=1}^{R_s}\sum_{n(r_s)=1}^{N(r_s)}E_{v,p}^{tot}(x_{n(r_s)},y_{n(r_s)})\Omega_{n(r_s)}(x,y) \tag{7}$$

by minimizing at each step *s* the *Multiple-Frequency Multi-Resolution Cost Function* defined as follows

$$\Psi^{(s)}=\frac{\sum_{p=1}^{P}\sum_{v=1}^{V}\sum_{m_{v,p}=1}^{M_{v,p}}\left|E_{v,p}^{scatt}(x_{mv,p},y_{mv,p})-\Theta_{v,p}^{ext}\left[\tau_{ref,s}(x_{n(r_s)},y_{n(r_s)}),E_{v,p,s}^{tot}(x_{n(r_s)},y_{n(r_s)})\right]\right|^2}{\sum_{p=1}^{P}\sum_{v=1}^{V}\sum_{m_{v,p}=1}^{M_{v,p}}\left|E_{v,p}^{scatt}(x_{mv,p},y_{mv,p})\right|^2}+ \\ \frac{\sum_{p=1}^{P}\sum_{v=1}^{V}\sum_{r_s=1}^{R_s}\sum_{n(r_s)=1}^{N(r_s)}w(x_{n(r_s)},y_{n(r_s)})\left|E_{v,p}^{inc}(x_{n(r_s)},y_{n(r_s)})-E_{v,p,s}^{tot}(x_{n(r_s)},y_{n(r_s)})+\Theta_{v,p}^{\mathrm{int}}\left[\tau_{ref,s}(x_{n(r_s)},y_{n(r_s)}),E_{v,p,s}^{tot}(x_{n(r_s)},y_{n(r_s)})\right]\right|^2}{\sum_{p=1}^{P}\sum_{v=1}^{V}\sum_{r_s=1}^{R_s}\sum_{n(r_s)=1}^{N(r_s)}\left|E_{v,p}^{inc}(x_{n(r_s)},y_{n(r_s)})\right|^2} \tag{8}$$

where $w(x_{n(r_s)},y_{n(r_s)})$ is a weighting function [12] and $N(R_s)=\max_p\{N_p\}$.

3. Numerical Results

This section gives some preliminary results obtained by the *IMSA-FH* and by the *IMSA-MF* techniques as well as a comparison with the reconstruction with the standard monochromatic approach (in the following, indicated as *IMSA-SF*). The selected test case [Fig. 3(*a*)] consists of a layered cylindrical structure centred at $x_c^{ref}=-y_c^{ref}=0.7\lambda$ (λ being the wavelength at $f=7GHz$) in a square investigation domain $L_{D_i}=3.5\lambda$-sided. The inner square layer ($L_{in}=0.35\lambda$ in side) is characterized by $\tau_{in}=0.5$, while the value of object function of the outer layer ($L_{in}=1.05\lambda$-sided) is equal to $\tau_{out}=2.0$. The investigation domain has been illuminated by a set of incident *TM*-polarized plane waves impinging from $V=8$ equally-spaced directions and the multi-frequency data ($P=3$, $f_1=5GHz$, $f_2=6GHz$, $f_3=7GHz$) have been synthetically generated in a set of measurement points located on a circle 3.5λ in radius. Moreover, the data have been blurred by adding a Gaussian noise characterized by $SNR=20dB$.

Because of the different information content available at each frequency [9], $M_{v,1}=31$, $M_{v,2}=37$, and $M_{v,3}=44$ field samples have been taken into account at f_1, f_2 and f_3, respectively. Consequently, $N_1=121$, $N_2=144$, and $N_3=169$ basis functions have been used for the *IMSA-FH* and the IMSA-SF), while $N(R_s)=N_3$, $s=1,...,S$, has been chosen for the *IMSA-MF* inversion.

The gray-level representations shown in Figs. 3(*b*)-(*d*) allow a preliminary comparative analysis among the proposed techniques. As a reference result, Fig. 3(*b*) shows a selected reconstruction processing through the *IMSA-SF* the measurement dataset at $f=7GHz$. Successively, the profile under test has been retrieved processing the $P=3$ available frequencies datasets with the multi-resolution frequency hopping approach

(*IMSA-FH*) [Fig. 2(*c*)]. As it can be noticed, the *IMSA* slightly takes advantage of the frequency hopping scheme, since the error figures [12] turn out to be $\chi_{tot}^{IMSA-SF} = 1.01\chi_{tot}^{IMSA-FH}$, $\chi_{\text{int}}^{IMSA-SF} \approx \chi_{\text{int}}^{IMSA-FH}$ and $\chi_{ext}^{IMSA-SF} = 1.32\chi_{ext}^{IMSA-FH}$.

Eventually, the *IMSA-MF* inversion scheme has been considered. The distribution of the reconstructed contrast shown in Fig. 3(*d*) points out that the use of multi-frequency data improve the accuracy in the retrieval of the outer as well as of the inner layer as quantitatively confirmed by values of the error figures ($\chi_{tot}^{IMSA-SF} = 2.22\chi_{tot}^{IMSA-MF}$, $\chi_{\text{int}}^{IMSA-SF} = 1.20\chi_{\text{int}}^{IMSA-MF}$, and $\chi_{ext}^{IMSA-SF} = 1.58\chi_{ext}^{IMSA-FH}$).

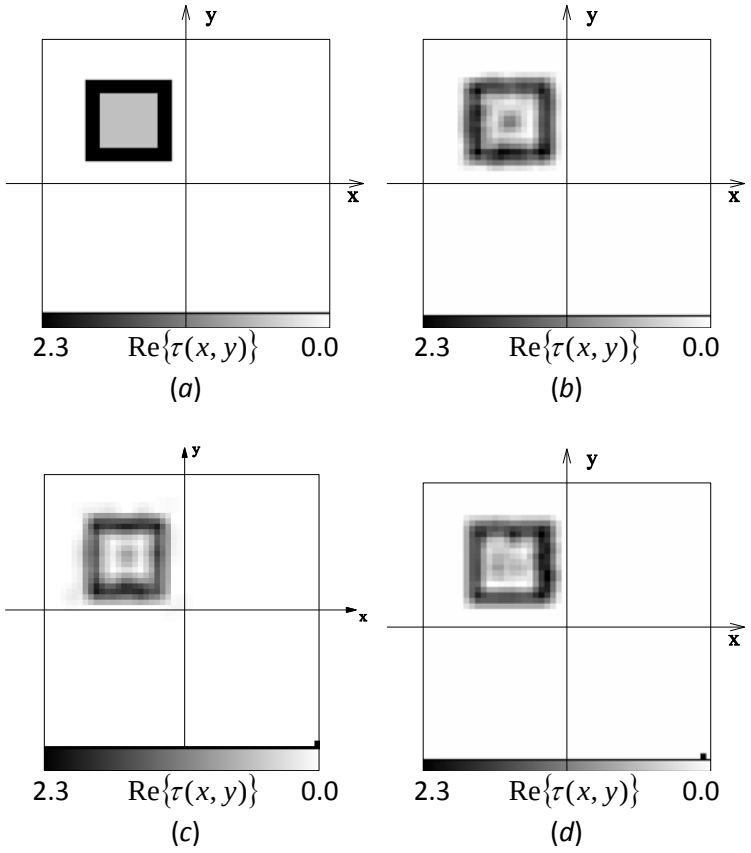

Figure 3. Layered Square Cylinder. (*a*) Reference distribution of the object function. Reconstruction obtained with by means of the (*b*) IMSA-SF, the (*c*) IMSA-FH and the (*d*) IMSA-MF.

4. Conclusions

A preliminary comparative assessment of two multi-resolution approaches for dealing with multi-frequency data has been carried out for evaluating potentialities and limitations of the proposed inversion algorithms. The achieved results have shown that the scheme based on the *IMSA-MF* may provide an enhanced reconstruction accuracy when processing multi-frequency information. However, further studies are needed in order to verify the robustness of the approach versus both the choice and the number of the illumination frequencies as well as its effectiveness and reliability in facing with real data.

References

[1] D. J. Daniels, *Subsurface Penetrating Radar*. London, U. K.: IEE Press, 1996.

[2] Y. Yu, T. Yu, and L. Carin, “Three-dimensional inverse scattering of a dielectric target embedded in a lossy half-space,” *IEEE Trans. Geosci. Remote Sensing*, vol. 42, pp. 957-973, 2004.

[3] P. M. Meaney, M. W. Fanning, D. Li, S. P. Poplack, and K. D. Paulsen, "A clinical prototype for active microwave imaging of the breast," *IEEE Trans. Microwave Theory Tech.*, vol. 48, pp. 1841-1851, Nov. 2000.

[4] J. M. Sill and E. C. Fear, "Tissue sensing adaptive radar for breast cancer detection - Experimental investigation of simple tumors models," *IEEE Trans. Microwave Theory Tech.*, vol. 53, pp. 3312-3319, Nov. 2005.

[5] O. M. Bucci and G. Franceschetti, "On the degrees of freedom of scattered fields," *IEEE Trans. Antennas Propagat.*, vol. 37, pp. 918-926, Jul. 1989.

[6] S. Caorsi, G. L. Gragnani, and M. Pastorino, "An approach to microwave imaging using a multiview moment method solution for a two-dimensional infinite cylinder," *IEEE Trans. Microwave Theory Tech.*, vol. 39, pp. 1062-1067, Jun. 1991.

[7] O. S. Haddadin and E. S. Ebbini, "Imaging strongly scattering media using a multiple frequency distorted Born iterative method," *IEEE Trans. Ultrason. Ferroelect. Freq. Contr.*, vol. 45, pp. 1485-1496, Nov. 1998.

[8] K. Belkebir, R. Kleinmann, and C. Pichot, "Microwave imaging - Location and shape reconstruction from multifrequency data," *IEEE Trans. Microwave Theory Tech.*, vol. 45, pp. 469-475, Apr. 1997.

[9] O. M. Bucci, L. Crocco, T. Isernia, and V. Pascazio, "Inverse scattering problems with multifrequency data: reconstruction capabilities and solution strategies," *IEEE Trans. Geosci. Remote Sensing*, vol. 38, pp. 1749-1756, Jul. 2000.

[10] A. G. Tijhuis, K. Belkebir, A. C. S. Litman, ans B. P. de Hon, "Theoretical and computational aspects of 2-D inverse profiling," *IEEE Trans. Geosci. Remote Sensing*, vol. 39, pp. 1316-1330, Jul. 2001.

[11] A. Baussard, "Inversion of multi-frequency experimental data using an adaptive multiscale approach", *Inverse Problems*, vol. 21, pp. S15-S31, Dec. 2005.

[12] S. Caorsi, M. Donelli, D. Franceschini, and A. Massa, "A new methodology based on an iterative multiscaling for microwave imaging," *IEEE Trans. Microwave Theory Tech.*, vol. 51, pp. 1162-1173, Apr. 2003.

[13] S. Caorsi, M. Donelli, and A. Massa, "Detection, location, and imaging of multiple scatterers by means of the iterative multiscaling method," *IEEE Trans. Microwave Theory Tech.*, vol. 52, pp. 1217-1228, Apr. 2004.